PHYSICAL REVIEW B **79**, 100403(R) (2009)

Oxygen-vacancy-induced ferromagnetism in CeO_2 from first principles

Xiaoping Han,[1] Jaichan Lee,[1,*] and Han-Ill Yoo[2]
[1]*School of Advanced Materials Science and Engineering, SungKyunKwan University, Suwon 440-746, Korea*
[2]*Department of Materials Science and Engineering, Seoul National University, Seoul 151-744, Korea*
(Received 14 October 2008; revised manuscript received 8 January 2009; published 10 March 2009)

The electronic and magnetic properties of CeO_2 with various concentrations of oxygen vacancies have been studied by first-principles calculations within the LSDA+U method and were found to remarkably depend on the oxygen vacancy concentration. With increasing oxygen deficiency, the electrons left behind by oxygen removal not only localize on Ce 4f orbitals but also on the vacancy sites. This leads to the magnetic mechanism with both superexchange and polarization in the cases of heavy doping, effectively enhancing the stability of ferromagnetism. The study reveals the magnetic properties and associated magnetic mechanisms of CeO_2 with the different oxygen deficiencies.

DOI: 10.1103/PhysRevB.79.100403 PACS number(s): 75.50.Pp, 61.72.Bb, 71.15.Mb

Global environment and energy issues have led to great interest in ceria (CeO_2) and related compounds, which can be applied to environmentally friendly power generation, such as solid oxide fuel cell and catalytic applications.[1–4] CeO_2 is known to be an oxygen vacancy reservoir with a high capacity for storing and releasing oxygen vacancies. Such a high oxygen vacancy storage capacity is essential in a wide variety of applications. To this end, oxygen vacancy often plays a vital role in changing materials properties, further influencing oxide-based device characteristics and reliability. For example, the high performance of CeO_2 as an oxygen buffer and active support for noble metals in catalysis relies on an efficient supply of lattice oxygens at reaction sites governed by oxygen vacancy formation.[5,6] Moreover, CeO_2 is widely used for ionic conducting oxides due to the role of oxygen vacancy.

It is well known that the stoichiometrical CeO_2 is paramagnetic. When an oxygen atom is released from CeO_2, two electrons are left behind and are believed to strongly localize at the f-level traps on two Ce atoms, which causes the formal valence of two neighboring Ce atoms to change from +4 to +3. This will give rise to net spin in the Ce f states, inducing the magnetism. However, little effort has been done to study the magnetic properties of oxygen-deficient CeO_2. Furthermore, most previous studies have been limited to slightly reduced CeO_2, while CeO_2 is known to be an effective oxygen vacancy reservoir. In fact, high oxygen deficiency in CeO_2 is a very likely situation in a wide range of applications since the oxides are often exposed to various environments, such as a highly reducing atmosphere or a high-temperature condition. In this study, we therefore have examined the localization behavior of CeO_2 with various degrees of oxygen deficiency as well as the associated magnetic properties and their origins. This study reveals that the electrons are localized not only on the Ce 4f state but also on the oxygen vacancy site (i.e., the electron localization tendency on the Ce 4f state weakens) when the oxygen deficiency becomes large. These electrons remaining on the oxygen vacancy site are polarized by the reduced ions, eventually leading to the evidently enhanced ferromagnetic ordering in highly oxygen deficient CeO_2.

First-principles methods, implemented in the Vienna *ab initio* simulation package (VASP),[7] were used to study the electronic and magnetic properties of CeO_{2-x}, particularly, the effects of oxygen vacancy doping concentration (x=3.13%, 6.25%, 12.5%, and 25% corresponding to $2\times2\times2$, $1\times2\times2$, $1\times1\times2$, and $1\times1\times1$ supercells with one oxygen vacancy, respectively). In all calculations, the projector augmented wave method (PAW) (Ref. 8) with the frozen-core approximation was used for the ion-electron interactions. Exchange correlation interactions were described by the PAW local spin density approximation (LSDA). Due to the strong Coulomb interaction of the localized Ce 4f electrons, the standard density-functional theory (DFT) calculations were inadequate for a satisfactory electronic structure prediction. Many recent reports[9–12] have proven that DFT calculation with the correction of Hubbard U parameter (DFT+U) is effective for CeO_{2-x} and related compounds. Dudarev's spherical LDA+U methods[13] were employed in this study. The optimal combination of U=8 eV and J=1 eV for Ce 4f orbitals was found to improve the prediction of the electronic structure. The Brillouin-zone (BZ) integration was performed on a well-converged Monkhorst-Pack k-point grid. The plane-wave kinetic energy cutoff was set to be 400 eV. Atomic positions and lattice parameters were optimized until the atomic forces were smaller than 0.02 eV/Å.

First, a $CeO_{1.969}$ supercell was used to model a low doping concentration case (x=0.0313), where one oxygen atom is removed from a 96-atom $2\times2\times2$ supercell of pure CeO_2. Figure 1(a) shows the total density of states (DOS) of $CeO_{1.969}$. The peak just below the Fermi level represents the localized f states, which are mainly on two Ce ions that are the nearest neighbors to the O vacancy. The gap between the O 2p valence-band edge and occupied f state is 1.4 eV, which agrees well with the experimental value of 1.2–1.5 eV.[14] Figures 1(b)–1(d) show the total DOSs of CeO_{2-x} (x=0.0625, 0.125, and 0.25). The existence of the gap states in these figures reveals the electron localization. These localized states are also due to the 4f states of the reduced Ce ion, originating from the electrons by oxygen removal. The integration analysis using Bader analysis[15] shows that each of the two reduced Ce ions has 0.98, 0.97, 0.93, and 0.91 electrons for the cases of x=0.0313, 0.0625, 0.125, and 0.25,

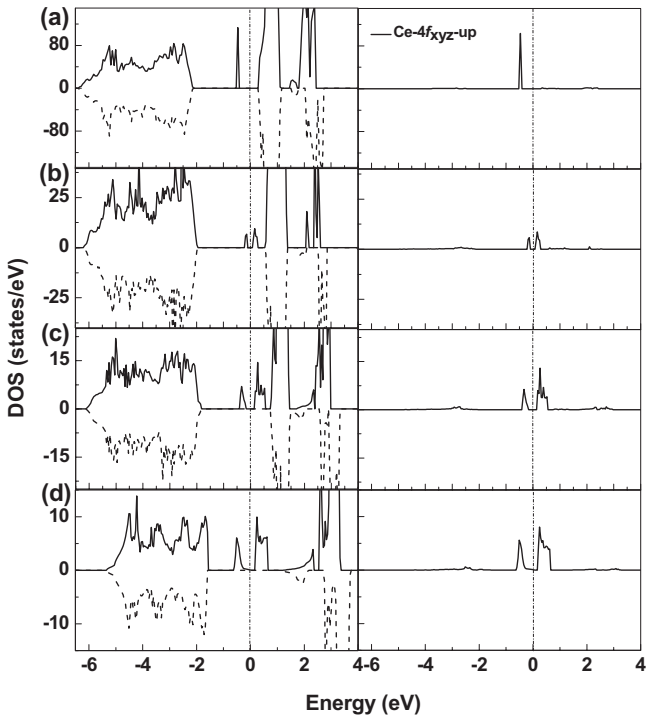

FIG. 1. Total DOS (left panel) and partial DOS (right panel) of $4f_{xyz}$ orbital (spin up) of two reduced Ce ions in CeO_{2-x} with (a) $x=0.0313$, (b) 0.0625, (c) 0.125, and (d) 0.25. The Fermi level is at zero in energy.

respectively. Therefore, two excess electrons are mostly transferred to two neighboring Ce^{4+} ions that are reduced to Ce^{3+} (each with $4f^1$ configuration). Those results were confirmed by the valence-band photoemission,[14] where a state appears in the energy gap between the top of the valence band and the bottom of the unoccupied Ce $4f$ band for the partially reduced ceria system. Further decomposition shows that these gap states are mostly due to f_{xyz} orbitals, meaning that the electrons from oxygen vacancy doping mostly occupy the f_{xyz} orbitals, as shown on the right panel of Fig. 1.

Interestingly, the followings were noticed in the localization behavior. First, with the increasing O-vacancy concentration, the gap states split into full and empty states. It is attributed to the large electron density originating from the heavy oxygen deficiency, which leads to strong electron correlation enough to split the impurity band.[16] Second, the localization behavior at a high oxygen deficiency differs from that at a low oxygen deficiency, although two electrons are mostly transferred to two Ce^{4+} ions in all four doping cases. As shown above, the amount of electrons localized on the Ce $4f$ state decreases with the increasing vacancy concentration. In other words, the electron density left behind on the oxygen vacancy site increases with oxygen vacancy concentration. The integration analysis shows that 0.13 and 0.16 electrons remain on the vacancy sites in the cases for $x=0.125$ and 0.25, respectively. Therefore, the gap states have substantial contributions from the electrons on the oxygen vacancy site in the case of high oxygen deficiencies. To further elucidate this localization behavior, the charge-density analysis of the gap state in the case of $x=0.25$ was performed, as shown in Fig. 2. It is clear that there are substantial electrons on the site of the oxygen vacancy, though most of the doped electrons occupy the Ce sites.

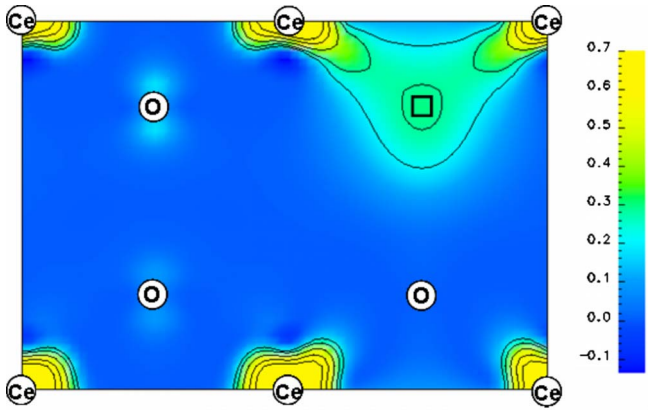

FIG. 2. (Color online) The charge-density analysis of the gap state in Fig. 1(d). The (110) plane through the two reduced Ce ions and O vacancy is chosen, and oxygen vacancy is represented as the solid square. The contour goes from 0.2 to 0.6 $e/Å^3$ in intervals of 0.1 $e/Å^3$.

The total energies of the ferromagnetic (FM) and antiferromagnetic (AFM) orderings were examined. The energy differences between FM and AFM orderings [$\Delta E = E(\mathrm{FM})\text{-}E(\mathrm{AFM})$] were −6, −11, −43, and −57 meV/cell for the cases of $x=0.0313$, 0.0625, 0.125, and 0.25, respectively, indicating that the FM state was more stable than the AFM state. Those theoretical results are supported by an experimental report,[17] where the oxygen vacancy induced ferromagnetism was observed in CeO_2. Furthermore, it should be noted that CeO_{2-x} showed an evidently enhanced stability of ferromagnetism as the oxygen deficiency increases. Several vacancy configurations, such as cluster and ordered states, and the variation in their stability were allowed in the calculations. The different vacancy configurations had little effect on the ferromagnetic state and did not influence the magnetic behavior, i.e., the enhanced stability of FM ordering with the oxygen vacancy concentration.

It is generally accepted that the electronic spins of cations in insulating oxides are normally coupled by the superexchange interactions through nonmagnetic ions, i.e., the superexchange interaction between neighboring magnetic ions via an anion.[18] In oxygen-deficient CeO_2, two electrons from oxygen vacancy occupy the $4f_{xyz}$ orbitals of two Ce ions. These two reduced Ce ions form a Ce-O-Ce bond with their neighboring oxygen anion, where Ce $4f_{xyz}$-O $2p$-Ce $4f_{xyz}$ interaction is responsible for the magnetic properties, as shown in Fig. 3. Goodenough-Kanamori-Anderson (GKA) rules[19,20] were adapted to the superexchange process of the f-electron system (two reduced Ce ions via oxygen ion). In Ce $4f_{xyz}$-O $2p$-Ce $4f_{xyz}$ interaction where one electron occupies the Ce $4f_{xyz}$ orbital of the reduced Ce ions, the Ce-O-Ce bond angle is close to 90° (ranging from 118 to 111° with the corresponding oxygen deficiency from $x=0.0313$ to 0.25). Figure 3 shows the Ce $4f_{xyz}$ orbital symmetry relative to the

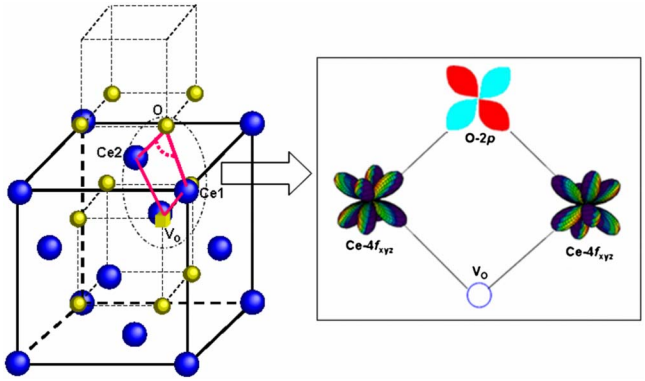

FIG. 3. (Color online) Schematic for the superexchange interaction between two reduced Ce ions. Ce1 and Ce2 represent the two reduced Ce ions. The Ce1-O-Ce2 superexchange is responsible for both light- and heavy-doping cases, while the interaction between Ce1 and Ce2 via V_O is effective only for the heavy-doping case.

O $2p$ orbital, which favors 90° superexchange interaction, leading to ferromagnetic ordering. The process of superexchange interaction is shown in Fig. 4. Similar results appear in the doped transition-metal oxides,[21] where the systems have ferromagnetic ordering due to 90° superexchange interaction.

It is well known that the superexchange interaction depends strongly on the electron occupancy, the orbital configuration, and the metal-anion-metal bond angle. As the interaction has the same orbital configuration of Ce ions (Ce $4f_{xyz}$), the similar electron occupancy on Ce $4f_{xyz}$ and similar bond angle for the different oxygen deficiencies, the magnetism originating from the superexchange interaction with the Ce $4f_{xyz}$-O $2p$-Ce $4f_{xyz}$ bond is not responsible for the evidently enhanced stability of the ferromagnetic state at the heavy doping. The main difference between the light- and heavy-doping cases is the increasing amounts of electrons remaining on the oxygen vacancy sites with the oxygen deficiency. Once the ferromagnetic ordering becomes stable through the Ce $4f_{xyz}$-O $2p$-Ce $4f_{xyz}$ superexchange interaction, the electrons are in turn polarized by the spin moment of neighboring Ce^{3+} ions under the ferromagnetic ordering. The partial DOS results showed that both electrons on the Ce $4f$ orbital and the oxygen vacancy are in a spin-up state. Moreover, the electrons on the oxygen vacancy sites would be involved in the Ce $4f_{xyz}$-V_O-Ce $4f_{xyz}$ superexchange interaction for ferromagnetic ordering. Based on the calculations and comparisons between the superexchange interaction and spin-polarization energy, the variations in the spin-polarization energy with oxygen deficiency were much larger than that of the superexchange interaction, suggesting that the enhanced ferromagnetism predominantly originates from the polarized electrons on the oxygen vacancy sites by ferromagnetic ordering of the reduced Ce ions. A similar idea was also proposed for the ferromagnetism in HfO_2.[22] Therefore, unlike the case of light doping where the ferromagnetism only originates from the superexchange, the superexchange and the polarization cooperatively underlie the ferromagnetism in heavy doping, explaining why the stability of ferromagnetism in the heavy doping is enhanced and

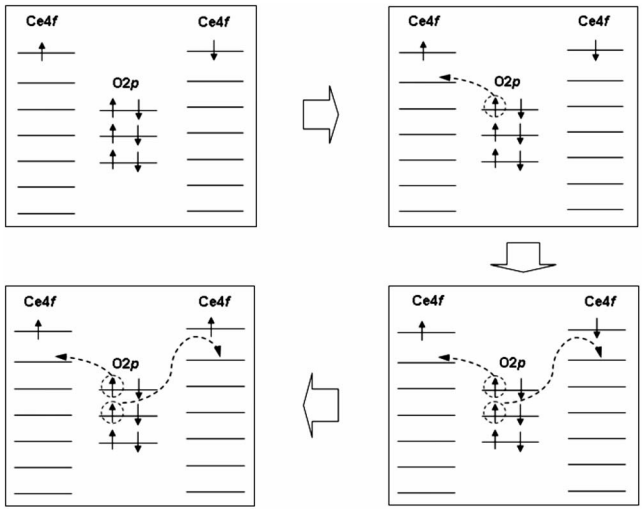

FIG. 4. Schematic of superexchange process between two reduced Ce ions via O^{2-} ion. First, one electron in one O $2p$ orbital is excited to $4f$ orbital of one Ce ion, and its spin direction is parallel to the electron on Ce $4f$ orbital based on Hund's rule. Because of the Ce-O-Ce bond angle close to 90°, the electron of the same spin in another O $2p$ orbital will be exchanged to $4f$ orbital of another Ce ion. This causes the $4f$ electron of the second Ce ion to have the parallel spin to that exchanged O $2p$ electron. Thus, the magnetic moments of two Ce ions are parallel to each other, leading to ferromagnetic coupling.

how the oxygen vacancy affects the magnetic states.

The importance of the occupancy of the electrons on the $4f_{xyz}$ orbitals of two Ce ions upon oxygen removal should be stressed. As shown in Fig. 3, the strongly directional configuration of the $4f_{xyz}$ orbital lobes provides a condition, where two Ce ions not only interact with their neighboring O $2p$ orbitals but also with the electrons on the oxygen vacancy sites. This $4f_{xyz}$ orbital symmetry leads to achievement of both the superexchange interaction and the polarization. If the electrons occupy other orbitals of the Ce $4f$ state, the superexchange and polarization may be not simultaneously involved. In fact, the crystal field of CeO_2 is of fundamental importance, where the occupancy of electrons on $4f_{xyz}$ orbitals is most stable. For other f-electron systems with the different crystal structures, orbitals other than $4f_{xyz}$ could be involved in the superexchange and spin polarization as long as electrons occupy the oxygen vacancy site. Similarly, in the d-electron system, the d orbitals involved must have an orbital symmetry favorable for the interaction with both oxygen ions and oxygen vacancies. To date, no such reports have been observed in the d-electron system.

In summary, the electronic and magnetic properties of oxygen-deficient CeO_2 have been studied using first-principles calculations within the LSDA+U method. The results show that the electronic structures and magnetic properties of CeO_2 heavily doped with oxygen vacancies are distinctly different from those with the light doping. With the increasing concentration of oxygen vacancies, the localized states induced by oxygen removal not only contain Ce $4f$ electrons but also receive substantial contribution from the electrons remaining on the vacancy sites. This localization

behavior effectively enhances the stability of ferromagnetism, which may be important in highly reducible *f*-electron oxide systems. Our study anticipates that a large concentration of oxygen vacancies plays an important role in the magnetic behavior of CeO_2.

This work was supported by the Korea Science and Engineering Foundation (KOSEF) through the National Research Laboratory (NRL) program and CAPST. The computations were carried out at KISTI through the Tenth Strategic Supercomputing Program.

*jclee@skku.edu

[1] *Catalysis by Ceria and Related Materials*, edited by A. Trovarelli (Imperial College Press, London, 1984).
[2] S. Park, J. M. Vohs, and R. J. Gorte, Nature (London) **404**, 265 (2000).
[3] G. A. Delug, J. R. Salge, L. D. Schmidt, and X. E. Verykios, Science **303**, 933 (2004).
[4] K. Otsuka, T. Ushiyama, and I. Yamanaka, Chem. Lett. **22**, 1517 (1993).
[5] F. Esch, S. Fabris, L. Zhou, T. Montini, C. Africh, P. Fornasiero, G. Comelli, and R. Rosei, Science **309**, 752 (2005); Q. Fu, H. Saltsburg, and M. Flytzani-Stephanopoulos, *ibid.* **301**, 935 (2003).
[6] Z. P. Liu, S. J. Jenkins, and D. A. King, Phys. Rev. Lett. **94**, 196102 (2005).
[7] P. E. Blochl, Phys. Rev. B **50**, 17953 (1994); G. Kresse and J. Furthmuller, *ibid.* **54**, 11169 (1996).
[8] G. Kresse and D. Joubert, Phys. Rev. B **59**, 1758 (1999).
[9] J. L. F. Da Silva, Phys. Rev. B **76**, 193108 (2007); J. L. F. Da Silva, M. V. Ganduglia-Pirovano, J. Sauer, V. Bayer, and G. Kresse, *ibid.* **75**, 045121 (2007).
[10] D. A. Andersson, S. I. Simak, N. V. Skorodumova, I. A. Abrikosov, and B. Johansson, Phys. Rev. B **76**, 174119 (2007); D. A. Andersson, S. I. Simak, B. Johansson, I. A. Abrikosov, and N. V. Skorodumova, *ibid.* **75**, 035109 (2007).
[11] C. W. M. Castleton, J. Kullgren, and K. Hermansson, J. Chem. Phys. **127**, 244704 (2007); Y. Jiang, J. B. Adams, and M. Schilfgaarde, *ibid.* **123**, 064701 (2005).
[12] M. Nolan, S. C. Parker, and G. W. Watson, Surf. Sci. **595**, 223 (2005); M. Nolan, S. Grigoleit, D. C. Sayle, S. C. Parker, and G. W. Watson, *ibid.* **576**, 217 (2005).
[13] S. L. Dudarev, G. A. Botton, S. Y. Savrasov, C. J. Humphreys, and A. P. Sutton, Phys. Rev. B **57**, 1505 (1998).
[14] M. A. Henderson, C. L. Perkins, M. H. Engelhard, S. Thevuthasan, and C. H. F. Peden, Surf. Sci. **526**, 1 (2003); D. R. Mullins, P. V. Radulovic, and S. H. Overbury, *ibid.* **429**, 186 (1999); A. Pfau, and K. D. Schierbaum, *ibid.* **321**, 71 (1994).
[15] G. Henkelman, A. Arnaldsson, and H. Jonsson, Comput. Mater. Sci. **36**, 354 (2006).
[16] S. Fabris, S. de Gironcoli, S. Baroni, G. Vicario, and G. Balducci, Phys. Rev. B **71**, 041102(R) (2005).
[17] Q. Wen, H. Zhang, Y. Song, Q. Yang, H. Zhu, and J. Xiao, J. Phys.: Condens. Matter **19**, 246207 (2007).
[18] J. B. Goodenough, *Magnetism and the Chemical Bond* (Interscience, New York, 1963).
[19] P. W. Anderson, Phys. Rev. **79**, 350 (1950); J. B. Goodenough, *ibid.* **100**, 564 (1955).
[20] J. Kanamori, J. Phys. Chem. Solids **10**, 87 (1959).
[21] R. Janisch and N. A. Spaldin, Phys. Rev. B **73**, 035201 (2006); X. Du, Q. Li, H. Su, and J. Yang, *ibid.* **74**, 233201 (2006).
[22] M. Venkatesan, C. B. Fitzgerald, and J. M. D. Coey, Nature (London) **430**, 630 (2004).